An automated online three-phase electro-extraction setup with machine-vision process monitoring hyphenated to LC-MS analysis

He, Y.; Miggiels, A.L.W.; Drouin, N.F.P.; Lindenburg, P.W.; Wouters, B.; Hankemeier, T.

Analytica Chimica Acta 1235 (2022) 340521

Contents lists available at ScienceDirect

Analytica Chimica Acta

journal homepage: www.elsevier.com/locate/aca

An automated online three-phase electro-extraction setup with machine-vision process monitoring hyphenated to LC-MS analysis

Yupeng He [a,1], Paul Miggiels [a,1], Nicolas Drouin [a], Peter W. Lindenburg [a,b], Bert Wouters [a,*], Thomas Hankemeier [a,**]

[a] Metabolomics and Analytics Center, Leiden Academic Centre for Drug Research, Leiden University, the Netherlands
[b] Research Group Metabolomics, Leiden Center for Applied Bioscience, University of Applied Sciences, Leiden, the Netherlands

HIGHLIGHTS

- An automated EE setup was integrated with a robotic autosampler coupled to LC-MS.
- The stability of EE process was assessed by machine vision and current monitoring.
- High enrichment factors up to 387 of the automated three-phase EE were achieved.
- Limits of detection were as low as 3.2 pg mL^{-1} in plasma samples.

GRAPHICAL ABSTRACT

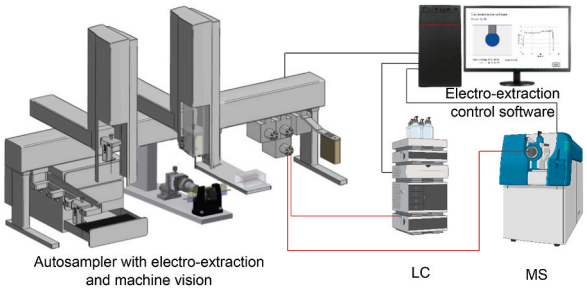

ARTICLE INFO

Keywords:
Electro-extraction
Automation
Machine vision
Sample preparation
Bioanalysis

ABSTRACT

Sample preparation is a labor-intensive and time-consuming procedure, especially for the bioanalysis of small-volume samples with low-abundant analytes. To minimize losses and dilution, sample preparation should ideally be hyphenated to downstream on-line analysis such as liquid chromatography-mass spectrometry (LC-MS). In this study, an automated three-phase electro-extraction (EE) method coupled to machine vision was developed, integrated with a robotic autosampler hyphenated to LC-MS. Eight model compounds, *i.e.* amitriptyline, clemastine, clomipramine, haloperidol, loperamide, propranolol, oxeladin, and verapamil were utilized for the optimization and evaluation of the automated EE setup. The stability of automated EE was evaluated by monitoring the acceptor droplet size by machine vision and recording the current during EE. A Design of Experiment approach (Box-Behnken design) was utilized to optimize the critical parameters of the EE method, *i.e.,* the ratio of formic acid in the sample to acceptor phase, extraction voltage, and extraction time. The developed quadratic models showed good fitness ($p < 0.001$, $R^2 > 0.95$). Automated EE could be achieved in less than 2 min with enrichment factors (EF) up to 387 and extraction recoveries (ER) up to 97% for academic samples. Finally, the optimized EE method was successfully applied to both spiked human urine and plasma samples with low-concentration (50 ng mL^{-1}) analytes and a low starting sample volume of 20 μL of plasma and urine in 10-fold diluted samples. The developed automated EE setup is easy to operate, provides a fast extraction method for analytes from volume-limited biological samples, and is hyphenated with on-line LC-MS analysis.

* Corresponding author. Einsteinweg 55, 2333 CC, Leiden, the Netherlands.
** Corresponding author.
E-mail addresses: b.wouters@lacdr.leidenuniv.nl (B. Wouters), hankemeier@lacdr.leidenuniv.nl (T. Hankemeier).
[1] These authors contributed equally to this paper.

https://doi.org/10.1016/j.aca.2022.340521
Received 4 August 2022; Received in revised form 7 October 2022; Accepted 12 October 2022
Available online 21 October 2022

Therefore, this method can provide fast and automated sample preparation to solve bottlenecks in high-throughput bioanalysis workflows.

1. Introduction

Sample preparation still poses a bottleneck for bioanalysis workflows of biomass-limited samples, *i.e.*, samples that are low in volume and/or have a low abundance of analytes [1–4]. Manual sample preparation is laborious and often time-consuming, which negatively affects its repeatability [5–8]. Alternative strategies must be considered to achieve consistently high extraction performance. This has been a driving force for the development of automated and hyphenated sample-preparation techniques that can clean up and preconcentrate analytes, can consistently handle small volumes, minimize solvent consumption, and can be directly hyphenated to analytical instrumentation such as liquid chromatography-mass spectrometry (LC-MS) or capillary electrophoresis – mass spectrometry to minimize sample loss [1,5,9–14].

Liquid-liquid extraction (LLE) and solid-phase extraction (SPE) are the most commonly used sample-preparation techniques [15–17]. However, both are labor- and time-consuming and use relatively large amounts of environmentally-unfriendly organic solvents, which in turn also results in the dilution of the analytes for small-volume samples. Electro-driven techniques are emerging as sample-preparation methods as they offer a simple extraction process that achieves simultaneous clean-up and high enrichment from biomass-limited samples [18–21]. Electro-driven extraction techniques can be categorized as supported liquid membrane electromembrane-extraction (SLM-EME) and free liquid membrane electro-membrane-extraction (FLM-EME), with the main difference being the presence of a solid membrane between the sample and acceptor [21]. Due to the absence of the solid membrane, FLM-EME is more straightforward in design, costs, and potential for

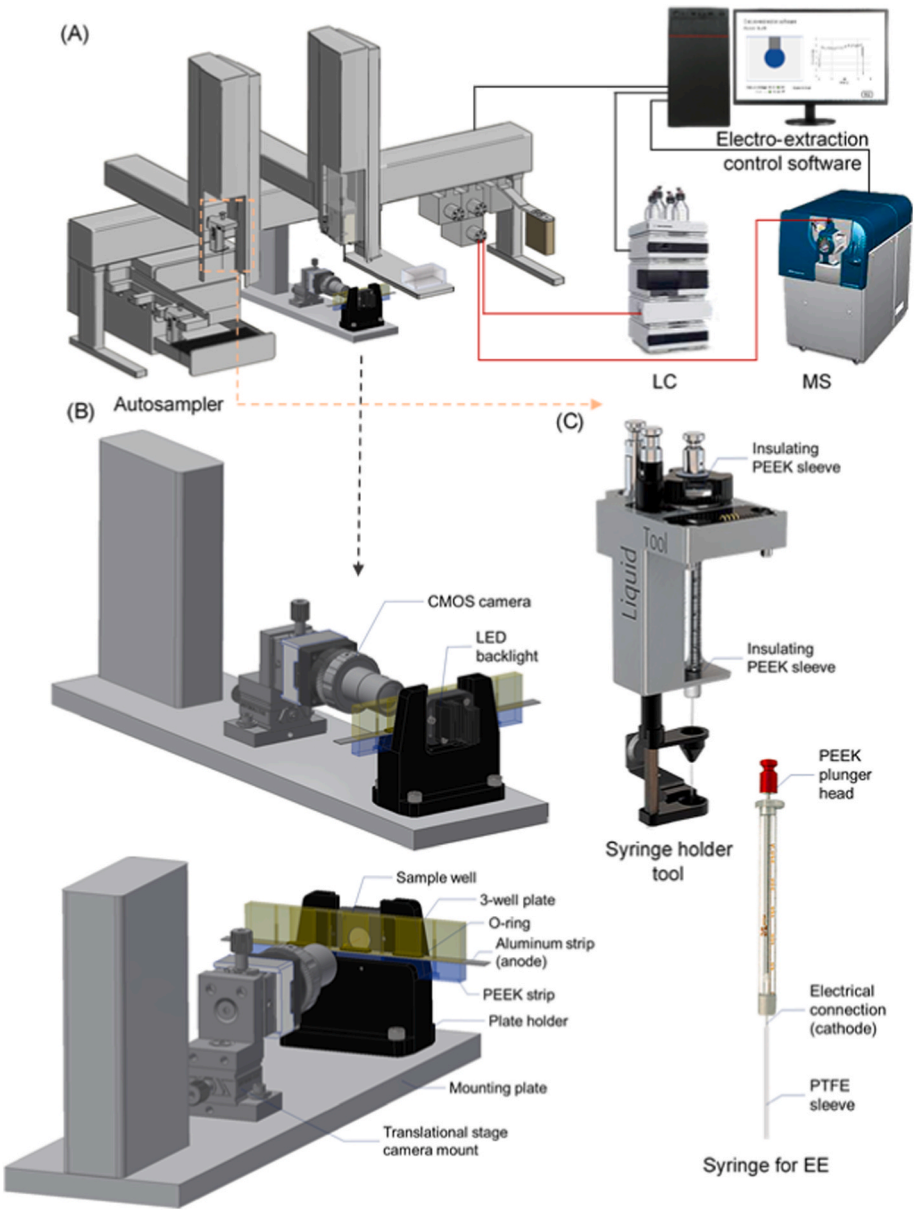

Fig. 1. Schematic diagram of the electro-extraction module integrated in the autosampler (A), details of the EE 3-well plate and imaging setup (B), and the modified syringe holder tool and the modified syringe for EE (C).

automation. Three-phase electro-extraction (EE) is a subtype of FLM-EME, with an aqueous acceptor droplet formed in the organic phase and was first reported by Raterink et al. in 2013 [22]. A single-droplet acceptor phase was widely used in the three-phase EE with the use of a digital camera to monitor the droplet status [14, 22–24]. However, the stability of the droplet during EE and the effect of this stability on EE are so far still unclear. The current during EE was also reported to monitor EE status [25], but its relation to EE performance still needs to be further investigated. Most electro-driven extraction methods reported so far are manually operated with little potential for automation [22–24,26–31]. Raterink et al. performed the three-phase EE on an automated nanoESI robot (Triversa NanoMate) that allowed for direct coupling to the mass spectrometer. However, this system could only be hyphenated offline to separation instruments, which would lead to the injection of a fraction of the extract [22].

The CTC PAL robotic autosampler is an established auto-sampler platform that provides flexibility for the integration of in-house developed setups and hyphenation to LC. To take profit from the high enrichment factors of three phase-EE, we have developed an automated on-line three-phase EE module on a CTC PAL robotic autosampler, hyphenated with LC-MS and equipped the module with machine vision – for acceptor droplet monitoring and volume calculation – and current monitoring. The ratio of formic acid (FA) in the sample to acceptor phase, extraction voltage, and extraction time were optimized by using an experimental design methodology (Box-Behnken design) for eight commonly-used model (basic and non-polar) compounds, namely amitriptyline, clemastine, clomipramine, haloperidol, loperamide, propranolol, oxeladin, and verapamil [24,27,32]. Finally, the optimized automated three-phase EE setup was successfully applied to human urine and plasma samples and the effect of protein precipitation on the performance of the method has been assessed. This study provided a stable automated three-phase EE setup hyphenated to LC-MS for low-volume, low-abundant samples that could alleviate the sample-preparation bottleneck in bioanalysis workflows.

2. Material and methods

2.1. Chemicals

Amitriptyline, clemastine, clomipramine, haloperidol, loperamide, propranolol, oxeladin, and verapamil were purchased from Sigma-Aldrich (Steinheim, Germany). MilliQ water was obtained from a Millipore high-purity water dispenser (Billerica, MA, USA). Formic acid and acetic acid were purchased from Acros Organics BVBA (Geel, Belgium). Ethyl acetate and acetonitrile were purchased from Biosolve Chimime SARL (Dieuze, France). All solvents were HPLC grade or higher.

2.2. Standard and sample solutions

Stock solutions of all model compounds (100 μg mL^{-1}) were prepared in 1:1 MeOH: H_2O (v/v) and stored at 4 °C. Prior analysis, academic samples were prepared by diluting stock solutions to a concentration of 500 ng mL^{-1} in the desired percentage of formic acid (FA) in MilliQ water. To evaluate the method in human plasma and urine samples, 50 ng mL^{-1} of amitriptyline, clemastine, clomipramine, haloperidol, loperamide, propranolol, oxeladin, and verapamil were spiked to undiluted, 5-fold, and 10-fold diluted urine and plasma (with and without protein precipitation) samples. Freshly pooled urine samples were obtained from adult, healthy volunteers (age 27 to 32). EDTA-treated plasma samples (obtained from Sanquin, Leiden, The Netherlands) were kept frozen at −80 °C until analysis and were thawed at room temperature only directly before use. The model compounds were spiked in urine and plasma samples before dilution and/or protein precipitation. For this, ice-cold MeOH was used for the protein precipitation of plasma samples with a ratio MeOH: plasma of 4:1, v/v [33]. The supernatant was evaporated to dryness using a SpeedVac Vacuum concentrator (Thermo Savant SC210A, Waltham, Massachusetts, United States) and reconstituted at the stated percentage of FA in water to the 1-, 5-, and 10-times dilution with regards to the starting volume.

2.3. Automated EE setup and extraction process

The automated extraction and subsequent injection was integrated on a CTC PAL3 RSI/RTC dual-headed robotic autosampler (CTC Analytics AG, Zwingen, Switzerland) (Fig. 1A), equipped with a 6-port VICI Cheminert Nanovolume vertical port injector valve with a 2-μL stainless steel loop (VICI AG, Schenkon, Switzerland) and a custom module for the electro-extraction process. The EE module (Fig. 1B) consisted of a support for a custom 3-well sample holder fitted with a LED backlight and a color CMOS camera (Basler dart daA1600-60UC; Basler AG, Ahrensburg, Germany) with a 2x zoom, 40 mm working distance telecentric lens (TechSpec® CompactTL™; Edmund Optics Ltd., York, United Kingdom), mounted to two translation stages to adjust the height and distance. All custom parts were designed and manufactured by the Fine Mechanical Department at Leiden University.

To clearly visualize the acceptor droplet, a transparent 3-well sample holder was used, which consisted of four parts that were screw-assembled, described from the top to bottom as follows: a 98 × 16 × 6 mm piece of cyclic olefin copolymer (COC) in which three oblong through-holes with a volume of 380 μL that was CNC milled (Haas OM2-A; Haas Automation Inc. Oxnard, CA, USA), ethylene propylene (EP) O-rings (0.9 mm diameter, 28.3 mm length; Apple Rubber Products Inc., Lancaster, NY, USA) for leak-tight sealing, a 1 mm strip of aluminum as an electrode, and an 8 mm strip of polyetheretherketone (PEEK) for rigidity and electrical insulation. The PEEK strip featured three sockets for a ball-detent locking mechanism for sideways alignment of the wells. COC was chosen for its optical transparency, chemical resistance to the solvents used, and good machinability.

The extraction was performed with a 10 μL glass syringe with a G22s needle (CTC Analytics AG, Zwingen, Switzerland) (Fig. 1C) that was fitted with a PEEK plunger head for electrical insulation and a polytetrafluoroethylene (PTFE) sleeve (1/32″ ID, 1/16” OD) around the lower part of the needle. Additional custom PEEK sleeves and insets were placed in the syringe tool holder to eliminate potential points of electrical contact between the syringe and the autosampler. The process voltage was supplied by a 0–1500 V DC high voltage power supply (RB10 1.5P, Matsusada Precision, Shiga, Japan) with an external 0–5 V DC control. Electrical connections were made with insulated clamps, one at the COC wells (anode) and one at the uncovered section of the syringe needle (cathode). Two additional resistors were placed in series with the process: a 10 MΩ current limiting resistor for operator safety, and a 100 kΩ shunt resistor to measure the process current. These values were chosen to minimally affect the process under the assumption that the process resistance exceeded 1 GΩ.

The extraction process was as follows: 200 μL of aqueous sample and 100 μL of organic phase (ethyl acetate saturated with MilliQ water) were transferred into a well; 6 μL of acceptor phase was aspirated in the modified 10 μL syringe; the syringe needle was lowered into the extraction well and a 0.5 μL acceptor droplet was formed at its tip; the extraction was started at the set voltage and time; the acceptor droplet was aspirated and subsequently injected in the injection valve towards the LC-MS. All samples and solvents were stored at 4 °C in the autosampler.

2.4. Automation

The CTC PAL3 autosampler was programmed and controlled with PAL Sample Control (PSC) 3.10 (CTC Analytics AG, Zwingen, Switzerland). The EE module was integrated into the autosampler as a general injector module with adjustable injection depth, and the depth was fixed after calibration. The extraction process was controlled by an in-house developed program created under LabView 2021 (National

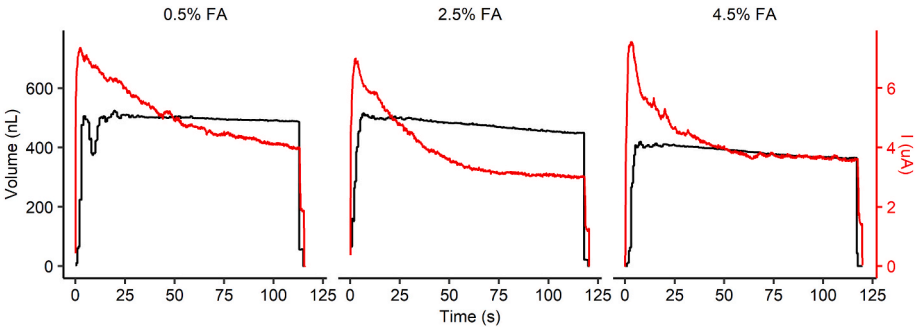

Fig. 2. Droplet volume (black color) and process current (red color) during the extraction of crystal violet at 150 V extraction voltage, 120 s extraction time, and various percentages of formic acid in the acceptor phase). (For interpretation of the references to color in this figure legend, the reader is referred to the Web version of this article.)

Instruments, Austin, Texas, USA) program that set the process voltage and timing, recorded the video of the process, and logged the process current to a file at a rate of 10 frames or measurements per second. An NI USB-6008 interface (National Instruments, Austin, Texas, USA) was used to synchronize with the autosampler via start/stop signals, provide 0–5 V control signal to the power supply, and monitor the process current. All parameters for the process such as droplet volumes, extraction voltage, and extraction time were entered in the PSC sample list and shared with the LabView program via a plaintext file.

2.5. LC-MS methods

The autosampler was coupled to an Agilent 1200 Series G1312B pump (Agilent, Waldbronn, Germany) and a Sciex 5600+ Triple-time-of-flight mass spectrometer (TripleTOF/MS; AB Sciex LLC), and a Synergi™ Phenomenex C18 LC column (50 × 2 mm, 4-μm particle size) kept at 40 °C with an Agilent 1200 Series G1316A column oven (Agilent, Waldbronn, Germany). The LC was used with an isocratic mobile phase composition of 60:40 water:acetonitrile with 0.1% acetic acid and a flow rate of 0.3 mL min^{-1}. The pump was controlled by Lab Advisor version B.02.07 (Agilent, Waldbronn, Germany). Source settings for the mass spec were set as follows: curtain gas 39.3 psi, source temperature 400 °C, ion source voltage 4.64 kV. Spectral data was acquired in full scan with a range of 100–1000 *m/z* and scan rate of 10 scans/s in positive ionization mode using Sciex Analyst 1.7 (AB Sciex LLC, Framingham, MA, USA). Peaks were extracted with mass accuracy of ±0.02 width and integrated with MultiQuant version 3.0.1 (AB Sciex LLC, Framingham, MA, USA).

2.6. Data analysis and calculation

Statistical analysis was carried out with SPSS (IBM Statistics 25). Design-Expert (version 12.0, Stat-Ease, Minneapolis, USA) was utilized for the optimization of the parameters of the three-phase EE by using a Box-Behnken design (BBD) of experiment. The enrichment factor (EF) [19,22,24] and extraction recovery (ER) [19,34] were calculated by Equations (1) and (2):

$$EF = \frac{(Analyte\ peak\ area\ in\ acceptor\ phase)_{after\ EE}}{(Analyte\ peak\ area\ in\ aqueous\ sample)_{before\ EE}} \quad \text{(Equation 1)}$$

$$ER(\%) = EF \times \frac{V_d}{V_s} \bullet 100\% \quad \text{(Equation 2)}$$

where V_d and V_s are the volumes of the acceptor droplet (0.5 μL) and the aqueous sample (200 μL), respectively.

To assess the stability of the droplet volume during extraction, the droplet volume was calculated from the recorded videos with a custom LabView program. Firstly, the needle region was selected for each video and an appropriate binarization threshold was determined. Then for each frame, the image was binarized, and connected holes in the drop and needle perimeter were filled. Next, the needle region was subtracted, and after hole-filling and particle removal, a binary matrix of the drop profile was obtained (Fig. S1). The drop volume was calculated from this using disc integration along the vertical axis, using the sum of each row as the diameter of the disc: $V_{droplet} = \frac{\pi}{4} d_{px}^3 \sum_{i=1}^{n} \sum_{j=1}^{n} x_{ij}^2$, in which is d_{px} the known size of a square pixel of 2.25 μm.

3. Results and discussion

Firstly, the performance of the developed automated EE setup was evaluated by the stability of the acceptor droplet size, as calculated by the machine vision system, and the current monitored during the EE procedure. Subsequently, the parameters of the three-phase EE were optimized and the optimal extraction method was applied to plasma and urine samples.

3.1. Evaluation of the developed setup performance

The electro-extraction process was first evaluated visually by extracting 1 μg mL^{-1} of the cationic dye crystal violet (Video S1). The acceptor droplet colored dark blue from the extracted dye within seconds after starting the extraction and the droplet remained stable for over 120 s. This was repeated for various concentrations of formic acid and the droplet volume, and the process current were used to assess the stability and progress of the EE process. Fig. 2 shows that the acceptor droplet volume remained stable, *i.e.* does not fluctuate during the process, but marginally declines during the process. This could be caused by electrolysis of crystal violet at the droplet surface [35], which reduces the color intensity and hinders detection of the droplet interface for the volume calculation. The current decreased during the extraction process, more swiftly initially and then more gradually during the later phase of the process. The rate of decrease was slower for lower percentages of FA, which is supported by the theory (Equations (3) and (4)) that a high flux (J_i) and current (I) can be obtained with low ion balances (χ) [25,32,36].

$$J_i = \frac{-D_i}{h}\left(1 + \frac{v}{\ln \chi}\right)\left(\frac{\chi - 1}{\chi - \exp(-v)}\right)(C_{ih} - C_{i0}\exp(-v)) \quad \text{(Equation 3)}$$

Supplementary data related to this article can be found at https://doi.org/10.1016/j.aca.2022.340521.

3.2. Method optimization

3.2.1. Optimization model design and model quality

The operational EE parameters were optimized to maximize the enrichment factor using a Box-Behnken design (BBD). Based on the theoretical model of the analyte flux (J_i) in Equation (3) [25], the total extraction can be increased by modulating the analyte flux (J_i). J_i can be most easily improved by increasing the applied voltage (increasing v) or

Table 1
Investigated parameters for the Box-Behnken design.

Code level	A: FA% or ratio of FA in the sample to acceptor phase (2% FA in acceptor phase)	B: Voltage (V)	C: Extraction time (s)
−1	0.5% (0.25)	50	10
0	2.5% (1.25)	150	65
1	4.5% (2.25)	250	120

Note: Code −1, 0, and 1 were used to represent low, middle, and high levels of parameters.

decreasing the ion balance (χ) by altering the ratio of formic acid in the sample to the acceptor phase [25]. However, there is an antagonistic effect between extraction voltage and time, *i.e.*, an increase in extraction voltage limits the extraction time and vice versa [24,36]. Therefore, simultaneous optimization of the process was done with formic acid ratio (A), extraction voltage (B), and extraction time (C) as parameters.

A quadratic model was adopted in BBD, and seventeen experiments were conducted in triplicate with 5 center points. The investigating range for each parameter is listed in Table 1. The maximum voltage was set to 250 V because of the instability of the acceptor droplet at extraction voltages above this value. This maximum was determined as the voltage at which the acceptor droplet could be kept stable for at least 120 s.

Table 2 showed that the developed models were significant for all model compounds with $p < 0.001$. The lack of fit of these models was not significant with p-values larger than 0.06, demonstrating that the developed models fit well with the parameters utilized for optimization for all compounds. The statistical evaluation of the coefficients also revealed a good fit of the models with R^2 and adjusted R^2 above 0.95 and 0.88, respectively, for all model compounds. Overall, the developed models fit well with the experimental values for the subsequent method optimizations.

3.2.2. Optimization of the automated EE method

From the models, it followed that the optimal enrichment factors taking all analytes into account could be achieved with a formic acid ratio of 1.65 (3.3% in the sample, 2% in the acceptor phase), extraction voltage of 135 V, and extraction time of 98 s (Fig. 3, S2, and S3). When increasing the formic acid percentage from 0.5 to 3.3%, the increase in enrichment factors may be the contribution of increased buffer capacity and more stable pH during EE at a high formic acid percentage. However, the EF decreased again above the optimal FA percentage. A similar trend was also observed in our previous study [24]. The decline in the enrichment factor at higher percentage FA may be due to an overly high ion balance (χ) induced by the high cation concentration in the sample solution under these conditions [31,37].

Higher extraction voltage contributes to faster migration of the charged analytes during electro-extraction and therefore improves the extraction efficiency. However, for voltages over 135 V, the EF of the model compounds decreased (Fig. 3, S2, and S3). Similarly, the EF declined again after the optimal extraction time of 98 s (Fig. 3, S2, and S3). Similar results were also reported by Nojavan et al., in their case for extraction voltages and times over 20 V and 15 min [38], and 250 V and 20 min, respectively [39], and by Schoonen et al. for an extraction voltage over 300 V [40]. The decrease in enrichment above the optimum voltage and time could be attributed to excessive electrolysis [37,41–43]. Electrolysis in the cathode acceptor phase increases the pH of the acceptor phase, leading to a neutralization of the charge of the model compounds. This in turn reduces their polarity and increases back-extraction into the organic phase through a passive liquid-liquid extraction mechanism, which has been reported in numerous publications [18,22,24,28,37,43]. This was consistent with previous observations that there is an antagonistic effect between extraction time and voltage [24,36].

Under the optimal circumstances, the resulting EF of the academic samples ranges from 20 for propranolol to 387 for loperamide, and it showed a partial positive correlation with the polarity of the compounds, which was also observed in Ref. [22]. The low EF of propranolol may be due in part to it being more polar (logP = 3.0) than the other analytes (logP = 3.7–5.3), which affects solubility and migration through the organic phase [24]. The highest optimal EF of loperamide may be due to its higher lipophilicity (logP = 4.4) and larger pKa value (9.4), which improves its charge state and dissolution in the organic phase.

The optimum extraction time of 98 s is significantly faster than extraction times of 2.5–33.3 min reported in other studies [18,22,26,28–31,34,44,45]. This comparably short extraction time could be the combined contribution of higher extraction voltage, lower volume of the acceptor droplet, and higher surface-area-to-volume ratio of the near-spherical acceptor droplet. In comparison, the achieved EF (20.1–36.8) and recovery of 5.0–9.2% (Table S1) of amitriptyline, propranolol, and oxeladin, are lower than reported in our previous work (EF = 104.7–135.7, ER = 10–13%) [24]. This may be due to the bigger acceptor droplet (0.5 μL) used here compared to our previous study (0.25 μL) [24], which induced a lower enrichment during extraction, and the simultaneous optimization of the EE method for more model compounds with different polarity and charge status than the previous study. The longer optimal extraction time compared to our previous study may be due to the use of more relatively polar and less basic model compounds, *i.e.*, haloperidol and clomipramine, and the simultaneous optimization of the EE method for all of these compounds [24]. Under the optimal extraction conditions, the total time for the extraction is around 4 min, which was shorter compared to our previously-reported manual EE setup [23]. This includes the automated addition of the sample and organic solvent, forming, aspirating, and injecting the acceptor droplet, and finally cleaning the syringe.

Table 2
p-values and R^2 of response surface quadratic models for EF of the model compounds.

Source	Amitriptyline	Clemastine	Clomipramine	Haloperidol	Loperamide	Oxeladin	Propranolol	Verapamil
Model	<0.0001	<0.0001	0.0004	<0.0001	0.0009	0.0003	<0.0001	<0.0001
A: FA	0.0031	0.0244	0.0571	0.1511	0.0251	0.0835	0.0535	0.0460
B: Voltage	0.4583	<0.0001	0.0032	<0.0001	0.0773	0.0152	0.9216	0.0010
C: Time	<0.0001	<0.0001	<0.0001	<0.0001	<0.0001	<0.0001	<0.0001	<0.0001
AB	0.1126	0.2022	0.4166	0.3403	0.8572	0.2768	0.0701	0.0317
AC	0.4658	0.1067	0.1441	0.2074	0.4374	0.6532	0.9735	0.2294
BC	0.4027	0.4289	0.5059	0.2798	0.8874	0.1190	0.2309	0.0344
A^2	0.0043	0.0540	0.0637	0.1643	0.2163	0.0112	0.0798	0.1253
B^2	0.0003	<0.0001	0.0024	0.0005	0.0015	0.0315	0.0002	<0.0001
C^2	0.0006	<0.0001	0.0207	0.0013	0.0023	0.0292	0.0002	<0.0001
Lack of Fit	0.4994	0.2058	0.7622	0.2826	0.0913	0.0607	0.2836	0.6795
R^2	0.9877	0.9866	0.9619	0.9755	0.9509	0.9634	0.9875	0.9905
Adjusted R^2	0.9720	0.9693	0.9129	0.9439	0.8877	0.9163	0.9714	0.9784

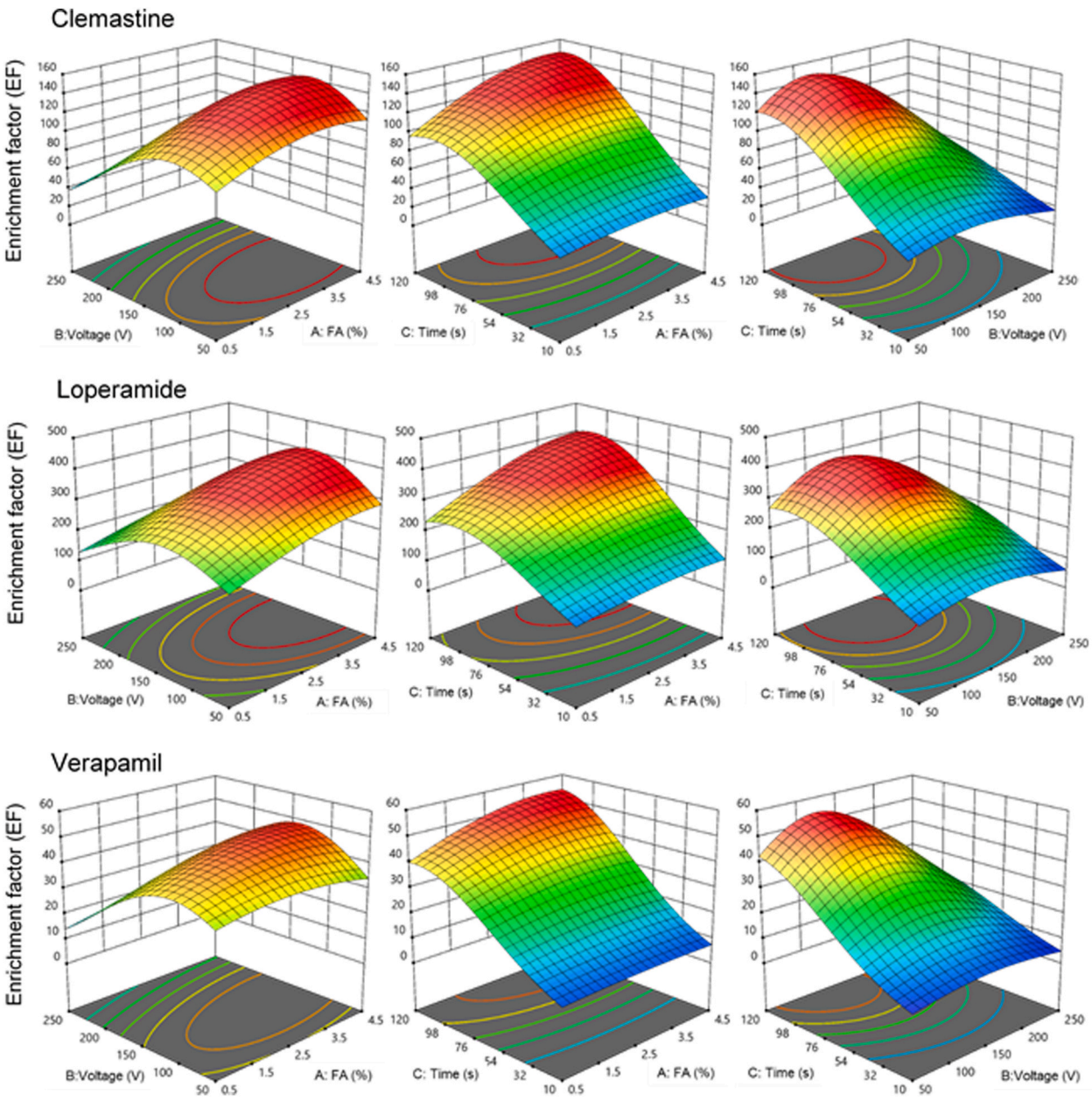

Fig. 3. Surface profiles of the developed quadratic models for representative model compounds, *i.e.*, clemastine, loperamide, and verapamil, as a function of extraction voltage and/or FA percentage or electro-extraction time at the optimum parameters.

3.3. Application and performance evaluation

To further investigate the applicability of the automated electro-extraction setup to biological samples, 50 ng mL^{-1} of analytes were spiked into human plasma and urine samples before diluting to 1-fold, 5-fold, and 10-fold of the starting volume. The influence of protein precipitation (PP) on plasma samples and the effect of a dilution on the PP samples were also investigated by spiking the model compounds before PP. As shown in Fig. 4, no significant difference in enrichment factor was observed between the undiluted, 5-fold, and 10-fold diluted plasma samples with PP in amitriptyline, haloperidol, oxeladin, and verapamil, suggesting that dilution has limited effect on the extraction performance when the samples are protein precipitated prior to the electro-extraction. However, in plasma samples without PP, the enrichment factor notably increased with dilution, and for clemastine, clomipramine, loperamide, and verapamil, the enrichment factor after 10-fold dilution was significantly higher ($p < 0.05$) than in undiluted samples. However, the gain in enrichment factor was less than the dilution factor, resulting in an overall dilution of the sample. Plausible causes are that dilution reduced the concentration of the proteins from the plasma presenting at the interface between the sample and the organic phase, which improved the migration of analytes from sample to acceptor droplet [23,24], and/or less ion suppression induced by the dilution. For all model compounds, the enrichment factor in plasma appeared to be lower after protein precipitation, which may be due to the protein binding of some compounds and loss of analytes during protein precipitation [46–52]. However, it also indicates that the optimized EE method is able to separate the molecules with high protein affinity from the proteins (in the samples without PP). For the urine sample, the enrichment factor was also notably higher ($p < 0.05$) for 10-fold diluted samples than for 5-fold diluted and/or undiluted samples, indicating the reduced ion suppression and/or improved performance of the extraction. The gain in enrichment factor however is small and does not offset the loss due to dilution. The higher enrichment factor of academic

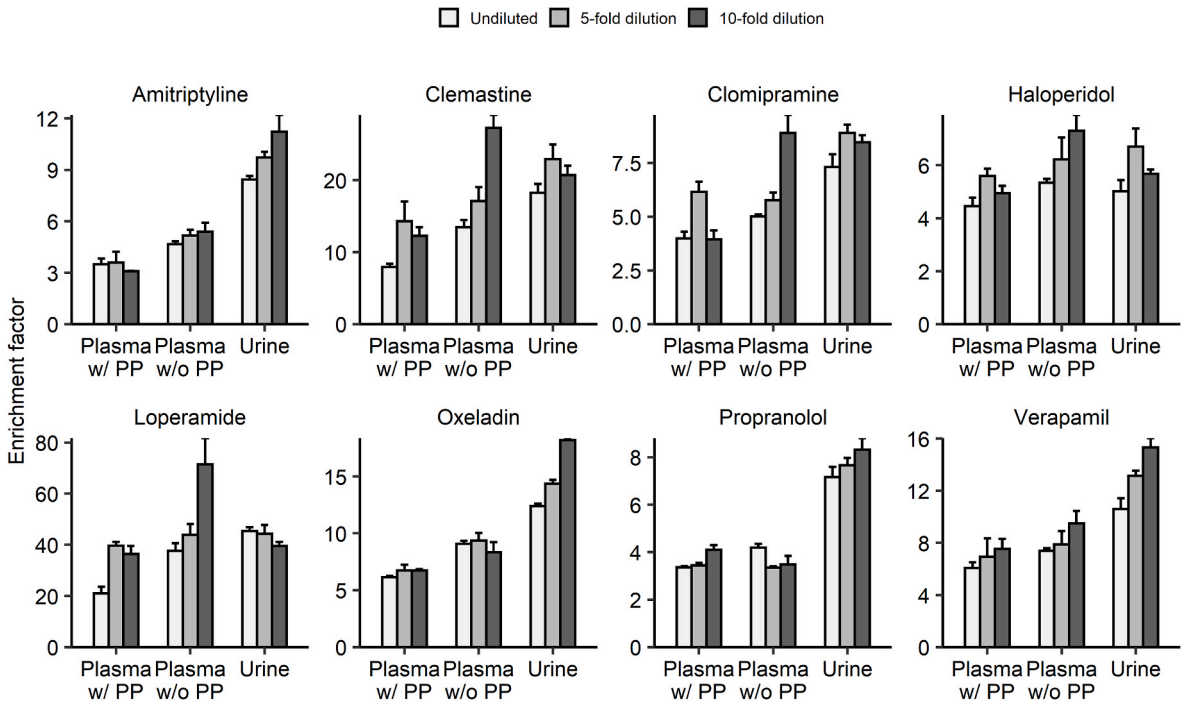

Fig. 4. The enrichment factor of model compounds spiked in undiluted, 5-fold and 10-fold diluted plasma, with protein precipitation (w/PP), without protein precipitation (w/o PP), and urine (n = 3).

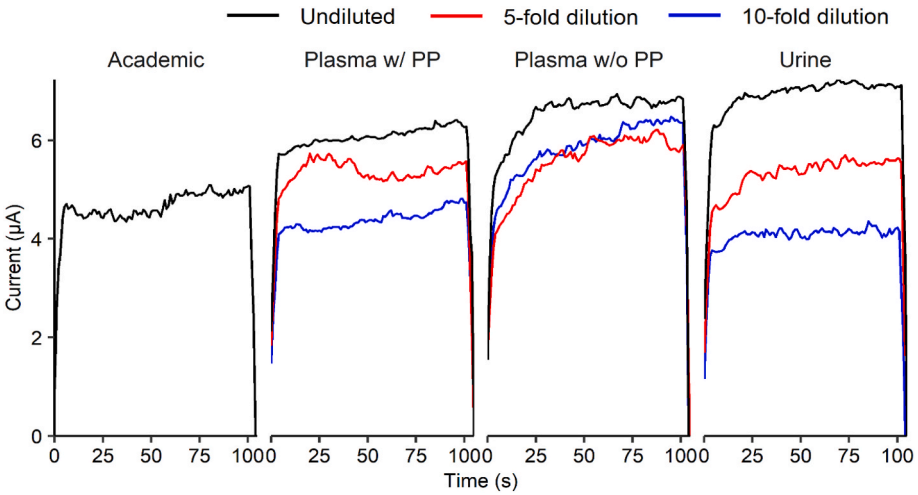

Fig. 5. The current monitored by optimal automated EE setup in undiluted, 5-fold, and 10-fold diluted urine, plasma with protein precipitation (w/PP), plasma without protein precipitation (w/o PP), and academic sample with optimal EE method.

samples (Table S1) compared to the enrichment factor of the biological (plasma and urine) samples was consistent with our previous work [24] and indicates that matrix effects occurred during the extraction process in biological samples. The enrichment factors in plasma and urine samples demonstrate a stable extraction process even with these matrix effects.

The current during electro-extraction of the biological samples was also recorded and shown in Fig. 5. A relatively more stable and constant current was measured during the extraction of urine and precipitated plasma compared to the non-precipitated plasma, and the average current level was reduced with an increased dilution factor. This observation is consistent with Equation (3), which describes that low cationic substance concentration in the sample solution (C_{ih}) obtained by dilution induces a lower flux (J_i), and further results in a lower current (Equation (4)). Babu et al. observed that higher protein concentration decreased sample conductivity and increased resistance [53], which is positively related to Joule heating. The increasing current in the non-precipitated plasma in Fig. 5 may be related to decreased conductivity, increased Joule heating, and increased temperature induced by higher protein concentrations. This is consistent with Gjelstad et al.'s theoretical model which indicates that increased temperature results in increased current during electro-extraction [25]. These current profiles differ from the initial spike in the current as observed with crystal violet (Fig. 2), which increased fast and then decreased gradually. This may be the contribution of the different concentration of crystal violet (1000 ng mL^{-1}) and non-optimal EE parameters used in Fig. 2. To explore the possible reasons for this difference, different concentrations of crystal violet were used for the current determination under the optimal EE method. The trend of a fast increasing and then decreasing current was observed in all concentrations of crystal violet, and this trend increased

Table 3
Calibration curve and precision (RSD) of the model compounds in the 10-fold diluted plasma and urine samples by using the optimized EE method (n = 3).

Matrix	Analyte	Linear range (ng mL^{-1})	Response function (R^2)	LOD(S/N = 3)(pg mL^{-1})	LOQ(S/N = 10)(pg mL^{-1})	Accuracy (%)	RSD (50 ng mL^{-1})	
						(25 ng mL^{-1})	Intraday	Interday
Plasma	Amitriptyline	10–1000	0.991	6.9	22.9	94	8.9%	1.5%
	Clemastine	10–1000	0.997	13.7	45.8	82	15.5%	19.3%
	Clomipramine	10–1000	0.995	25.0	83.4	91	5.7%	21.3%
	Haloperidol	10–1000	0.991	5.8	19.3	88	9.2%	11.2%
	Loperamide	10–1000	0.994	3.2	10.6	98	6.3%	16.7%
	Oxeladin	10–1000	0.997	4.9	16.5	109	10.9%	3.1%
	Propranolol	10–1000	0.991	7.3	24.2	128	12.5%	10.4%
	Verapamil	10–1000	0.995	7.5	25.1	89	1.0%	19.8%
Urine	Amitriptyline	10–1000	0.992	5.5	18.5	93	12.8%	11.9%
	Clemastine	10–1000	0.997	29.6	98.7	98	12.5%	8.0%
	Clomipramine	10–1000	0.990	29.7	99.1	92	10.1%	11.1%
	Haloperidol	10–1000	0.990	7.9	26.5	112	14.5%	9.9%
	Loperamide	10–1000	0.999	3.8	12.6	75	15.9%	10.3%
	Oxeladin	10–1000	0.990	5.8	19.3	119	2.3%	8.5%
	Propranolol	10–1000	0.990	7.5	24.9	107	8.2%	3.9%
	Verapamil	10–1000	0.990	8.9	29.8	106	9.0%	9.1%

with concentration (Fig. S4). The highest current value was observed in the highest crystal violet concentration (10000 ng mL^{-1}), which was consistent with Gjelstad et al.'s observation that a high initial analyte concentration in the sample solution strongly influenced the current and raised it to a high level [25]. The different current profile of crystal violet from the model compounds may be due to the easy charge and hydrophilic property of crystal violet.

Finally, the performance of the automated electro-extraction was evaluated by determining the response function, repeatability, limits of detection (LODs), limits of quantification (LOQs), and accuracy using the optimum extraction conditions with a small starting sample volume with 20 μL, *i.e.,* 10-fold diluted urine and plasma. All model compounds exhibited good linear response ($R^2 > 0.99$) within the concentration range from 10 to 1000 ng mL^{-1} (Table 3). The LODs and LOQs are in the range of 3.2–29.7 pg mL^{-1} and 10.6–99.1 pg mL^{-1}, respectively. The accuracy (75–128%), intra- and inter-day relative standard deviation (RSD) (<21%), and all the evaluated results demonstrate the stability, sensitivity, and repeatability of the EE method in both diluted plasma and urine samples. The automated extraction method also achieved better RSD and comparable accuracy (<12.8% and 93–128%, respectively) than our earlier manual procedure (<17.8% RSD and 73–107%, respectively) for the same compounds, *i.e.*, amitriptyline, oxeladin, and propranolol, from undiluted plasma and urine samples. This demonstrates that the automated EE setup provides better repeatability compared to the manual EE setup.

4. Conclusion

A fully integrated and automated three-phase electro-extraction, with machine vision control of the size of the hanging droplet, hyphenated to LC-MS, was developed and evaluated for stability and analysis of drugs in biofluids. The extraction was optimized with a Box–Behnken design methodology for eight model compounds, *i.e.* amitriptyline, clemastine, clomipramine, haloperidol, loperamide, propranolol, oxeladin, and verapamil. The results proved a stable and repeatable automated EE setup, achieving enrichment factors of 20–387 with an optimum extraction time of 98 s for academic samples. For application to human urine and plasma samples, the LODs were as low as 3.2 pg mL^{-1} from an equivalent of 20 μL of plasma, with a linear response function of $R^2 > 0.99$.

In summary, our one-step EE approach can simultaneously clean up and enrich samples prior to analysis in a short time and is well-suited for low-volume and low-concentration samples. Automation of this method provides a faster, more accurate, less laborious, and operator-safe method compared to our earlier manual electro-extraction setup. In future developments, the electro-extraction module can be modified to work with 96- or 384-well plates, for improvement of sample capacity and full integration with lab automation solutions, and can be applied to more analytes to further improve the application of the setup. We believe that this technique can provide an excellent solution for sample-preparation bottlenecks toward automated high-throughput bioanalysis workflows.

CRediT authorship contribution statement

Yupeng He: Investigation, Conceptualization, Formal analysis, Writing – original draft. **Paul Miggiels:** Investigation, Conceptualization, Writing – original draft. **Nicolas Drouin:** Conceptualization, Investigation, Writing – original draft. **Peter W. Lindenburg:** Conceptualization. **Bert Wouters:** Conceptualization, Supervision, Writing – review & editing. **Thomas Hankemeier:** Conceptualization, Supervision.

Declaration of competing interest

The authors declare that they have no known competing financial interests or personal relationships that could have appeared to influence the work reported in this paper.

Data availability

Data will be made available on request.

Acknowledgments

The authors are grateful to Emiel Wiegers, Raphaël Zwier, and Gijsbert Verdoes from the Fine Mechanical Department (FMD), and Raymond Koehler and Peter van Veldhuizen from the Electronics Department (ELD) at Leiden University for their contribution in developing the hardware and electronics of this setup. We thank Tom Vercammen from Interscience for discussions and suggestions during the development and integration of the electro-extraction setup in the CTC PAL autosampler. This work was supported by the Netherlands Organisation for Scientific Research (NWO) in the Building Blocks of Life (grant number 737.016.015); the China Scholarship Council (CSC) (No. 201706320322). Nicolas Drouin acknowledges the financial support from Horizon 2020 Marie Sklodowska-Curie CO-FUND (Grant Agreement No: 707404). This research was (partially) funded by the X-Omics project (Netherlands Organisation for Scientific Research, project No. 184.034.019).

Appendix A. Supplementary data

Supplementary data to this article can be found online at https://doi.org/10.1016/j.aca.2022.340521.

References

[1] L.G. Blomberg, Two new techniques for sample preparation in bioanalysis: microextraction in packed sorbent (MEPS) and use of a bonded monolith as sorbent for sample preparation in polypropylene tips for 96-well plates, Anal. Bioanal. Chem. 393 (2009) 797–807.

[2] J. Henion, E. Brewer, G. Rule, Sample preparation for LC/MS/MS: analyzing biological and environmental samples, Anal. Chem. 70 (1998) 650a–656a.

[3] R.N.X. Xu, L.M. Fan, M.J. Rieser, T.A. El-Shourbagy, Recent advances in high-throughput quantitative bioanalysis by LC-MS/MS, J. Pharmaceut. Biomed. Anal. 44 (2007) 342–355.

[4] R.J. Raterink, P.W. Lindenburg, R.J. Vreeken, R. Ramautar, T. Hankemeier, Recent developments in sample-pretreatment techniques for mass spectrometry-based metabolomics, Trac. Trends Anal. Chem. 61 (2014) 157–167.

[5] S. Mitra, Sample preparation techniques in analytical chemistry, J. Am. Chem. Soc. 126 (5) (2004), 1585-1585.

[6] B. Bojko, K. Gorynski, G.A. Gomez-Rios, J.M. Knaak, T. Machuca, V.N. Spetzler, E. Cudjoe, M. Hsin, M. Cypel, M. Selzner, M.Y. Liu, S. Keshavjee, J. Pawliszyn, Solid phase microextraction fills the gap in tissue sampling protocols, Anal. Chim. Acta 803 (2013) 75–81.

[7] M.A. Dineva, L. Mahilum-Tapay, H. Lee, Sample preparation: a challenge in the development of point-of-care nucleic acidbased assays for resource-limited settings, Analyst 132 (2007) 1193–1199.

[8] S.X. Peng, M. Cousineau, S.J. Juzwin, D.M. Ritchie, A 96-well screen filter plate for high-throughput biological sample preparation and LC-MS/MS analysis, Anal. Chem. 78 (2006) 343–348.

[9] D. Vuckovic, Current trends and challenges in sample preparation for global metabolomics using liquid chromatography-mass spectrometry, Anal. Bioanal. Chem. 403 (2012) 1523–1548.

[10] N. Drouin, S. Rudaz, J. Schappler, Sample preparation for polar metabolites in bioanalysis, Analyst 143 (2018) 16–20.

[11] P. Miggiels, B. Wouters, G.J.P. van Westen, A.C. Dubbelman, T. Hankemeier, Novel technologies for metabolomics: more for less, Trac. Trends Anal. Chem. 120 (2019), 115323.

[12] I. Kohler, J. Schappler, S. Rudaz, Microextraction techniques combined with capillary electrophoresis in bioanalysis, Anal. Bioanal. Chem. 405 (2013) 125–141.

[13] R. Pero-Gascon, F. Benavente, C. Neusüß, V. Sanz-Nebot, Evaluation of on-line solid-phase extraction capillary electrophoresis–mass spectrometry with a nanoliter valve for the analysis of peptide biomarkers, Anal. Chim. Acta 1140 (2020) 1–9.

[14] A. Oedit, B. Duivelshof, P.W. Lindenburg, T. Hankemeier, Integration of three-phase microelectroextraction sample preparation into capillary electrophoresis, J. Chromatogr. A 1610 (2020), 460570.

[15] A. Sarafraz-Yazdi, A. Amiri, Liquid-phase microextraction, Trac. Trends Anal. Chem. 29 (2010) 1–14.

[16] D.E. Raynie, Modern extraction techniques, Anal. Chem. 82 (2010) 4911–4916.

[17] Y.Y. Wen, L. Chen, J.H. Li, D.Y. Liu, L.X. Chen, Recent advances in solid-phase sorbents for sample preparation prior to chromatographic analysis, Trac. Trends Anal. Chem. 59 (2014) 26–41.

[18] A.Y. Song, J. Yang, Efficient determination of amphetamine and methylamphetamine in human urine using electro-enhanced single-drop microextraction with in-drop derivatization and gas chromatography, Anal. Chim. Acta 1045 (2019) 162–168.

[19] A. Oedit, R. Ramautar, T. Hankemeier, P.W. Lindenburg, Electroextraction and electromembrane extraction: advances in hyphenation to analytical techniques, Electrophoresis 37 (2016) 1170–1186.

[20] P.W. Lindenburg, R. Ramautar, T. Hankemeier, The potential of electrophoretic sample pretreatment techniques and new instrumentation for bioanalysis, with a focus on peptidomics and metabolomics, Bioanalysis 5 (2013) 2785–2801.

[21] N. Drouin, P. Kuban, S. Rudaz, S. Pedersen-Bjergaard, J. Schappler, Electromembrane extraction: overview of the last decade, Trac. Trends Anal. Chem. 113 (2019) 357–363.

[22] R.J. Raterink, P.W. Lindenburg, R.J. Vreeken, T. Hankemeier, Three-phase electroextraction: a new (online) sample purification and enrichment method for bioanalysis, Anal. Chem. 85 (2013) 7762–7768.

[23] Y. He, N. Drouin, B. Wouters, P. Miggiels, T. Hankemeier, P.W. Lindenburg, Development of a fast, online three-phase electroextraction hyphenated to fast liquid chromatography–mass spectrometry for analysis of trace-level acid pharmaceuticals in plasma, Anal. Chim. Acta 1192 (2022), 339364.

[24] Y. He, P. Miggiels, B. Wouters, N. Drouin, F. Guled, T. Hankemeier, P. W. Lindenburg, A high-throughput, ultrafast, and online three-phase electro-extraction method for analysis of trace level pharmaceuticals, Anal. Chim. Acta 1149 (2021), 338204.

[25] A. Gjelstad, K.E. Rasmussen, S. Pedersen-Bjergaard, Simulation of flux during electro-membrane extraction based on the Nernst-Planck equation, J. Chromatogr. A 1174 (2007) 104–111.

[26] N. Drouin, J.F. Mandscheff, S. Rudaz, J. Schappler, Development of a new extraction device based on parallel-electromembrane extraction, Anal. Chem. 89 (2017) 6346–6350.

[27] F.A. Hansen, E. Santigosa-Murillo, M. Ramos-Payan, M. Munoz, E.L. Oiestad, S. Pedersen-Bjergaard, Electromembrane extraction using deep eutectic solvents as the liquid membrane, Anal. Chim. Acta 1143 (2021) 109–116.

[28] L.E.E. Eibak, A. Gjelstad, K.E. Rasmussen, S. Pedersen-Bjergaard, Kinetic electro membrane extraction under stagnant conditions-Fast isolation of drugs from untreated human plasma, J. Chromatogr. A 1217 (2010) 5050–5056.

[29] L. Xu, P.C. Hauser, H.K. Lee, Electro membrane isolation of nerve agent degradation products across a supported liquid membrane followed by capillary electrophoresis with contactless conductivity detection, J. Chromatogr. A 1214 (2008) 17–22.

[30] L. Arjomandi-Behzad, Y. Yamini, M. Rezazadeh, Extraction of pyridine derivatives from human urine using electromembrane extraction coupled to dispersive liquid-liquid microextraction followed by gas chromatography determination, Talanta 126 (2014) 73–81.

[31] A. Slampova, P. Kuban, P. Bocek, Quantitative aspects of electrolysis in electromembrane extractions of acidic and basic analytes, Anal. Chim. Acta 887 (2015) 92–100.

[32] T.M. Middelthon-Bruer, A. Gjelstad, K.E. Rasmussen, S. Pedersen-Bjergaard, Parameters affecting electro membrane extraction of basic drugs, J. Separ. Sci. 31 (2008) 753–759.

[33] Y. Yang, C. Cruickshank, M. Armstrong, S. Mahaffey, R. Reisdorph, N. Reisdorph, New sample preparation approach for mass spectrometry-based profiling of plasma results in improved coverage of metabolome, J. Chromatogr. A 1300 (2013) 217–226.

[34] N. Drouin, S. Rudaz, J. Schappler, Dynamic-electromembrane extraction: a technical development for the extraction of neuropeptides, Anal. Chem. 88 (2016) 5308–5315.

[35] M. Abdi, M. Balagabri, H. Karimi, H. Hossini, S.O. Rastegar, Degradation of crystal violet (CV) from aqueous solutions using ozone, peroxone, electroperoxone, and electrolysis processes: a comparison study, Appl. Water Sci. 10 (2020) 168.

[36] S. Seidi, Y. Yamini, M. Rezazadeh, Electrically enhanced microextraction for highly selective transport of three β-blocker drugs, J. Pharm. Biomed. 56 (2011) 859–866.

[37] K.S. Hasheminasab, A.R. Fakhari, A. Shahsavani, H. Ahmar, A new method for the enhancement of electromembrane extraction efficiency using carbon nanotube reinforced hollow fiber for the determination of acidic drugs in spiked plasma, urine, breast milk and wastewater samples, J. Chromatogr. A 1285 (2013) 1–6.

[38] S. Nojavan, A. Pourahadi, S.S. Hosseiny Davarani, A. Morteza-Najarian, M. Beigzadeh Abbassi, Electromembrane extraction of zwitterionic compounds as acid or base: comparison of extraction behavior at acidic and basic pHs, Anal. Chim. Acta 745 (2012) 45–52.

[39] S. Nojavan, S. Asadi, Electromembrane extraction using two separate cells: a new design for simultaneous extraction of acidic and basic compounds, Electrophoresis 37 (2016) 587–594.

[40] J.W. Schoonen, V. van Duinen, A. Oedit, P. Vulto, T. Hankemeier, P. W. Lindenburg, Continuous-flow microelectroextraction for enrichment of low abundant compounds, Anal. Chem. 86 (2014) 8048–8056.

[41] C.X. Huang, A. Gjelstad, S. Pedersen-Bjergaard, Electromembrane extraction with alkylated phosphites and phosphates as supported liquid membranes, J. Membr. Sci. 526 (2017) 18–24.

[42] C.X. Huang, K.F. Seip, A. Gjelstad, S. Pedersen-Bjergaard, Electromembrane extraction of polar basic drugs from plasma with pure bis(2-ethylhexyl) phosphite as supported liquid membrane, Anal. Chim. Acta 934 (2016) 80–87.

[43] M. Balchen, A. Gjelstad, K.E. Rasmussen, S. Pedersen-Bjergaard, Electrokinetic migration of acidic drugs across a supported liquid membrane, J. Chromatogr. A 1152 (2007) 220–225.

[44] A. Wuethrich, P.R. Haddad, J.P. Quirino, Off-line sample preparation by electrophoretic concentration using a micropipette and hydrogel, J. Chromatogr. A 1369 (2014) 186–190.

[45] L. Arjomandi-Behzad, Y. Yamini, M. Rezazadeh, Pulsed electromembrane method for simultaneous extraction of drugs with different properties, Anal. Biochem. 438 (2013) 136–143.

[46] M.A. Levitt, J.B. Sullivan Jr., S.M. Owens, L. Burnham, P.R. Finley, Amitriptyline plasma protein binding: effect of plasma pH and relevance to clinical overdose, Am. J. Emerg. Med. 4 (1986) 121–125.

[47] H. Hansson, K. Bergvall, U. Bondesson, M. Hedeland, K. Torneke, Clinical pharmacology of clemastine in healthy dogs, Vet. Dermatol. 15 (2004) 152–158.

[48] A.E. Balantgorgia, M. Gexfabry, L.P. Balant, Clinical pharmacokinetics of clomipramine, Clin. Pharmacokinet. 20 (1991) 447–462.

[49] P. Morselli, G. Tedeschi, G. Bianchetti, J. Henry, R. Braithwaite, Plasma protein binding of haloperidol: influence of age and disease states, Psychiatr. Clin. Psychopharmacol. (1981) 191–196.

[50] K. Sadrjavadi, F. Rahmati, F. Jafari, S. Moradi, A. Nowroozi, M. Shahlaei, A study on the binding of loperamide to human serum albumin using combination of computational and experimental methods, Biochem. Anal. Biochem. 6 (2017), 1000346.

[51] W.R. Ravis, D.L. Parsons, S.J. Wang, Buffer and pH effects on propranolol binding by human albumin and α1-acid glycoprotein, J. Pharm. Pharmacol. J. 40 (2011) 459–463.

[52] D.L. Keefe, Y.G. Yee, R.E. Kates, Verapamil protein binding in patients and in normal subjects, Clin. Pharmacol. Ther. 29 (1981) 21–26.

[53] K.S. Babu, J.K. Amamcharla, Rehydration characteristics of milk protein concentrate powders monitored by electrical resistance tomography, JDS Communications 2 (2021) 313–318.